Chapter 5

Jindalee Radar Experimental Campaign

The CCP was designed to allow a wide variety of experiments at different field locations. In particular, the CCP permits the observation and capture of the temporal and spectral fading behaviour of radio signals propagating in the ionosphere.

As mentioned in the previous chapter, FMCW signals are ideal for the experimental study of fading of radio-waves propagating in the ionosphere. Their advantages include: good frequency and time resolution of the observed signal, ability to resolve multiple propagation modes, and lower susceptibility to random interference. However, a suitable transmitter that is capable of transmitting FMCW signal of significant power in the HF band is not widely available. Fortunately, the transmitter from the Jindalee OTHR was available for some of the experimental work in this project.

The purpose of this chapter is to give a detailed overview of the experimental campaign that utilised the Jindalee Radar. All important aspects of the experiment will be outlined. Furthermore, the signal processing involved in extracting useful information from the experimental data will be explained.

5.1 Rationale

To achieve the objectives of the experiment as outlined in Section 4.1, one must have suitable experimental apparatus and also a well designed experiment. Since the experiment was designed to investigate the different aspects of fading in radio signals propagating through the ionosphere, we have the following list of aims:

- Investigate the temporal and spectral fading behaviour of radio signals propagating in the ionosphere, and also how the fading behaves for the different modes of propagation over the same path.
- Determine how the fading behaviour correlates between two signals received by orthogonal antennas.
- Observe the various fading behaviour at different times of the day, and across different frequency channels.
- Discover the irregularity structures that are causing the different types of fading.

With the CCP on the receiver side taking advantage of dual-polarisation and the ability to observe multiple channels simultaneously, it is imperative to select a suitable transmission source, which includes the transmitter and the transmitted waveform, that has the following desirable features:

- Ability to transmit on multiple frequencies, at sufficient power such that it will not be affected by other transmitters in the HF band.
- Capable of containing not only a reasonably wide bandwidth in the HF band, but it must also contain sufficient temporal resolution.
- A transmitted waveform that is suitable for distinguishing the time delays from different modes of propagation over the same path.

The Jindalee OTHR transmitters have all the desirable characteristics for this experiment [78]. Through the help of the Defence Science and Technology Organisation (DSTO) it was possible to use the Jindalee OTHR transmitter located in Alice Springs.

5.2 Jindalee Over-The-Horizon Radar

The Jindalee Operational Radar Network (JORN) is a network of OTHR that provides air and sea surveillance across the vast coastline of the northern part of Australia [78]. OTHR works under the principle of HF skywave propagation in the ionosphere to achieve a surveillance and detection range of up to 3000 km. The JORN consists of three radars. Two radars are restricted to operational use, but the third, at Alice Springs, is available for research and development purposes. All radars are controlled from the JORN Coordination Centre (Edinburgh, South Australia) where all the data from the radar sites are processed.

The two main radar sites are the Longreach Radar (Radar 1) which has a 90° coveage and the Laverton Radar (Radar 2) which has a 180° coverage [78]. The third radar site is the Jindalee Facility Alice Springs (JFAS) Radar (1RSU) with a 90° coverage. JFAS radar continues to be operational after serving many years as the prototype and development site [79], and remains in its role as the radar for further research and development of the system while the other two sites are used for full-time operational purposes. It was the JFAS 1RSU radar transmitter that formed the basis of this experimental campaign. Figure 5.1 shows the locations of the sites and the coverage area of the three radars [80].

The JFAS radar transmitter, located at Harts Range (22.967° S, 134.448° E), employs a 28-element vertical polarised log-periodic antenna array. It is capable of transmitting on dual frequencies when operating in the "split radar" mode [78] that is ideal for monitoring fading on two channels simultaneously. Linear FMCW transmissions with variable bandwidths were transmitted, with the channels assigned by the Frequency Management System (FMS). The FMS collects the data from its various sub-systems, which include ionospheric condition data and HF spectrum occupancy information, and assigns the optimum channel and bandwidth for the operation of the radar [81]. This capability was exploited during the experiments to allocate the channels with the widest usable bandwidth.

Ionospheric conditions during the experimental periods were provided by the network of JORN ionosondes scattered across the northern parts of Australia [82]. The task of the ionosonde network is to provide real-time information on the ionospheric condition in support of JORN's radar operation. For the current experimental campaign, the ionosonde

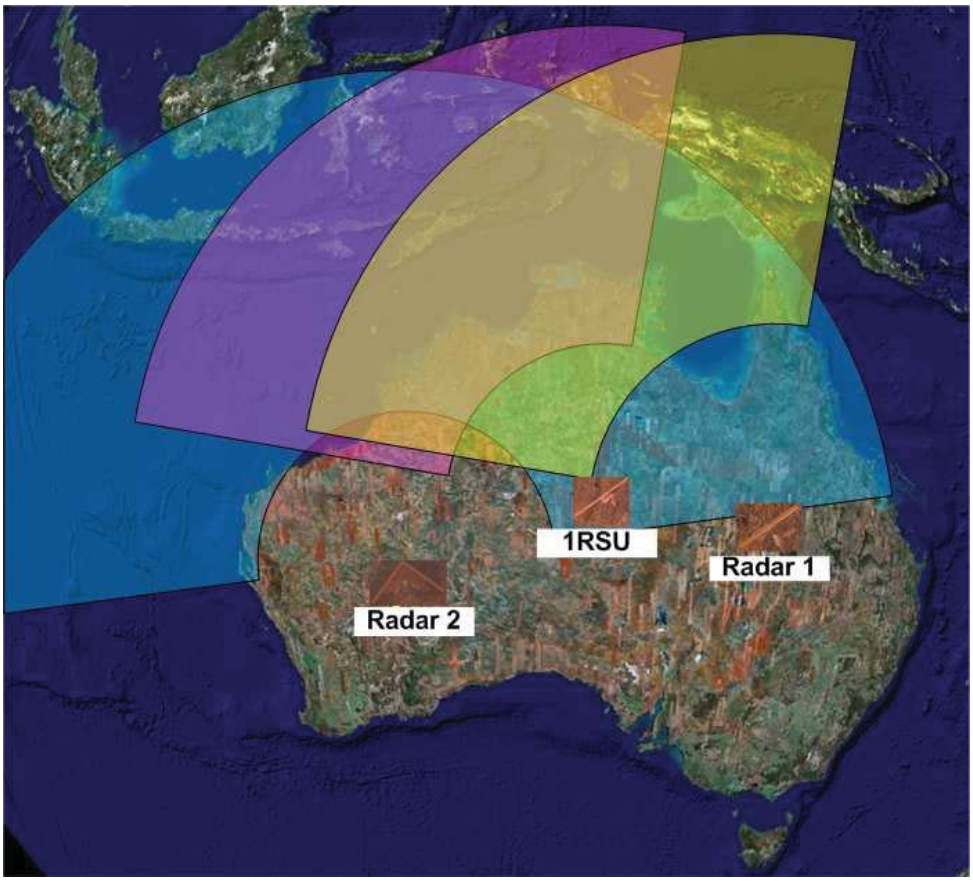

Figure 5.1. Map showing the three radar locations and their area of coverage. Radar 1 has a 90° coverage as shown in yellow, 1RSU has a 90° coverage as shown in magenta, and Radar 2 has a 180° coverage as shown in cyan.

data will be analysed to ascertain the types of ionospheric structure and irregularities that are causing the different types of fading.

5.3 Experimental Parameters

With the kind cooperation of DSTO, dedicated transmissions in the HF band for the sole purpose of this experiment were obtained from the JFAS radar transmitter. Data of the linear FMCW transmissions were collected over three days between the 29th to 31st of March 2005.

A station with the CCP was set up in Lake Bennett, 90km southeast of Darwin (12.962° S, 131.168° E), to receive the FMCW signal. The ground range between the

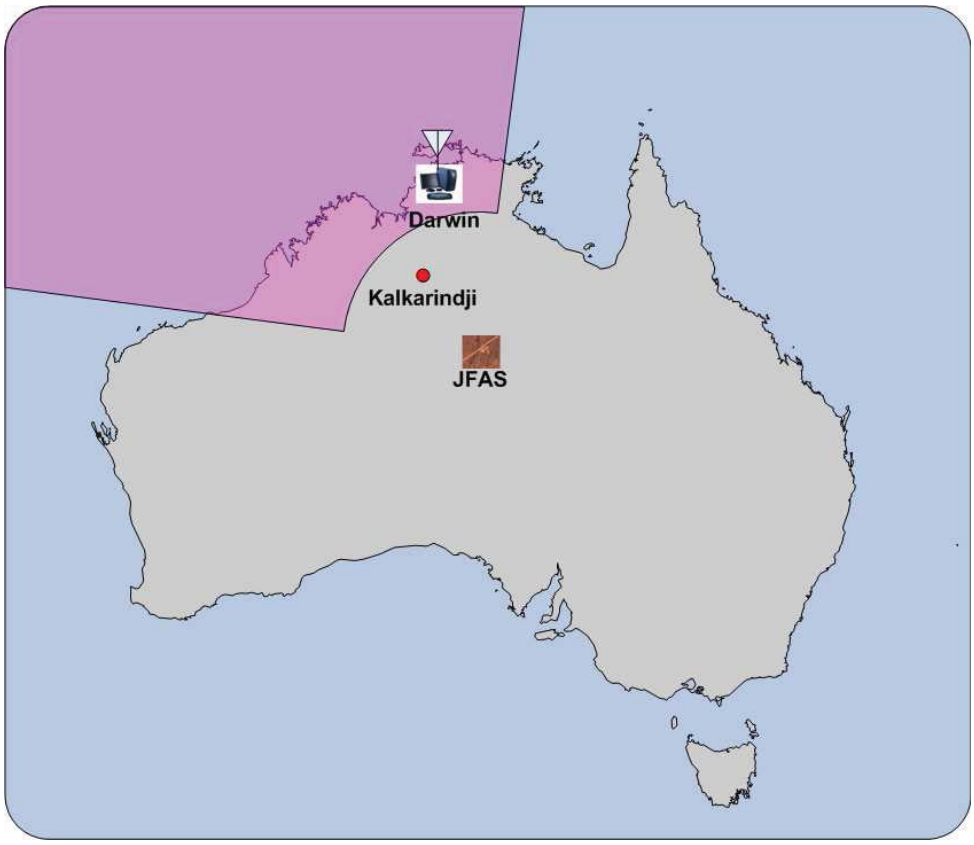

Figure 5.2. The location of the JFAS radar transmitter and the CCP in Darwin. Transmitter coverage is shown in magenta. Kalkarindji is the location of the ionosonde from which the ionospheric parameters of the path were recorded.

transmitter and the receiver was approximately 1200 km, of which the propagation path was almost in the north-south direction. Figure 5.2 shows the location of the transmitter and the receiver. There are two main reasons why this propagation path was chosen:

1. Lake Bennett is an accessible location within the illuminated range of the JFAS radar transmitter with the least amount of local man-made radio interference, and

2. The propagation path is almost aligned with the magnetic field. In such circumstance, energy is divided equally between the two magneto-ionic components, ordinary and extraordinary [83]. Furthermore, the O and X modes will be circularly polarised but opposite in direction. As such, the north-south propagation path will be the most susceptible to polarisation fading. With the dual-polarisations CCP, polarisation fading can be easily identified and would allow one to determine when polarisation fading is most dominant.

Date	Centre Frequency (MHz)	Bandwidth (kHz)	Start time (LT)	End time (LT)
29/03/2005	6.411	44	16:30	17:30
	13.212	50	16:30	17:30
	16.076	48	17:30	19:30
	17.328	60	17:30	19:30
30/03/2005	10.677	46	16:15	21:15
	10.858	44	16:15	21:15
31/03/2005	13.125	90	15:30	18:30
	14.951	46	15:30	18:30
	9.201	10	19:30	21:30
	9.281	10	19:30	21:30

Table 5.1. Centre frequencies and bandwidths of the linear FMCW signals that were transmitted during the 3-day experimental campaign.

Each day during the experiment, the radar transmitter was available from 15:30 until 21:30 local time. The centre frequency and bandwidth of the FMCW transmissions were based on the spectral availability at the time, as determined by the FMS. The available centre frequencies and the channel bandwidths for the duration of the experiment are shown in Table 5.1. The data collected on the second day of the experiment, 30 March 2005, forms the most important dataset because of the long duration of signal availability. Transmissions on the two channels, 10.677 MHz and 10.858 MHz, were sustained from the period of late afternoon to late evening with reasonably wide bandwidths. The long period of sustained transmission, together with ionosonde data, is ideal for studying the types of fading encountered at different times of the day.

5.4 Ionospheric Conditions

The propagation condition of the ionospheric channel is dependent on many factors. In particular it is heavily influenced by solar activities and disturbances of the magnetic fields around the Earth. Records of solar activities and magnetic disturbances over the three days were obtained to supplement the ionospheric parameters from the JORN ionosondes

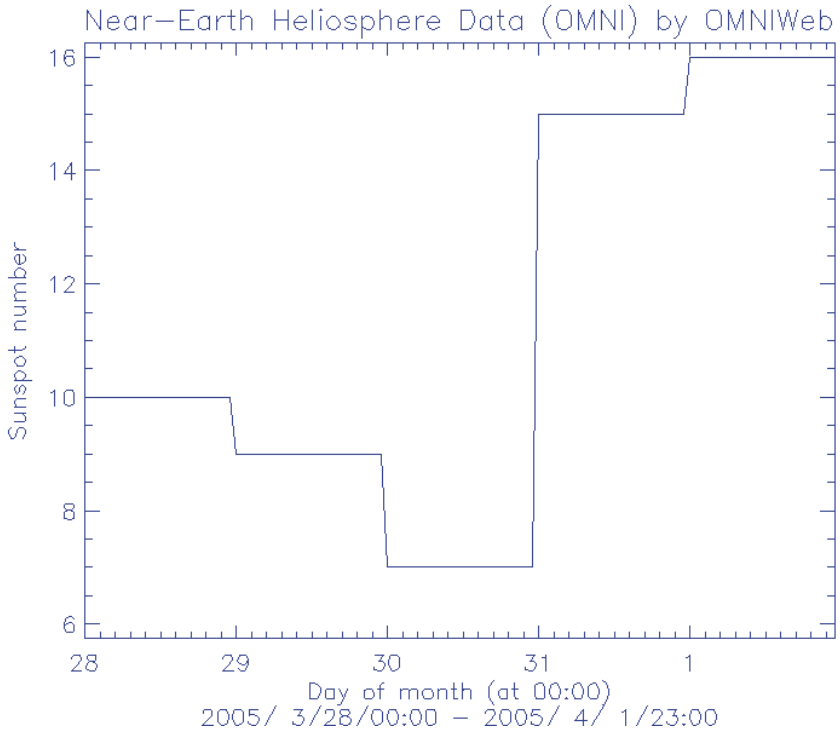

Figure 5.3. The global daily sunspot number over the period of 28 March 2005 to 1 April 2005.

to provide an accurate representation of the ionospheric structures and the irregularities during the experiment.

From the historical data, a correlation has been established between the critical frequencies of the F2 layer and the 11-year solar cycle where the sunspot activities, as measured by the sunspot number (SSN), go through a cycle of maximum and minimum over a 11-year period [84]. The daily value of SSN ranges from 0 up to 200 or more. The SSN measurement for the experimental period is shown in Figure 5.3. It shows low values of SSN during the experiments, which is expected since 2005 was approaching the trough of the 11-year solar cycle. As a consequence, the critical frequencies of the F2 layer will expected to be in the lower range of the scale.

Disturbances in the Earth's magnetic field are also important factors when considering the propagation conditions of the ionospheric channel, as ionospheric storms are often associated with heavily disturbed magnetic fields in the atmosphere. A common index that is used to measure the severity of the magnetic disturbance is the K_p index, which is a 3-hour global average of magnetic indices, with 0 representing quiet conditions and 9 representing extremely disturbed conditions. Figure 5.4 shows the K_p index multiplied

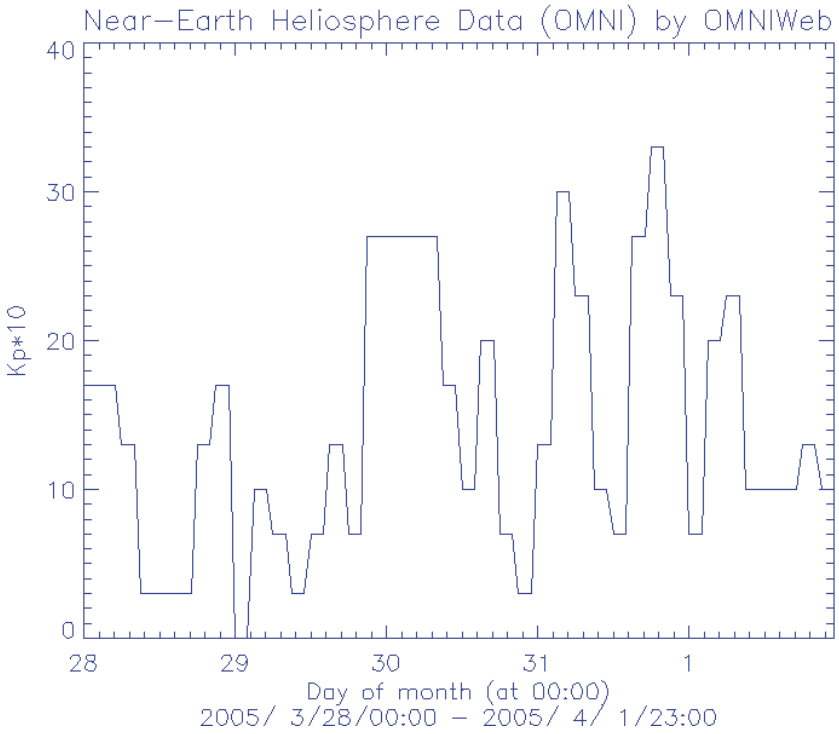

Figure 5.4. The global three-hour magnetic activity index, $10 \times K_p$, over the period of 28 March 2005 to 1 April 2005. The full-scale of 0 to 100 represents quiet magnetic conditions to extremely disturbed magnetic conditions.

by 10 (for a range of 0 to 100) over the three days of experiment. It is evident that the magnetic field conditions were relatively quiet with no occurrence of a magnetic storm.

5.4.1 Ionosonde Data

Ionospheric parameters such as critical frequencies and peak heights were obtained from the JORN ionosonde sounder located in Kalkarindji (17.44° S, 130.83° E). The vertically incident sounder in Kalkarindji was chosen due to its proximity to the midpoint of the propagation path where the ionospheric conditions would be most relevant for the 1-hop transmission path. Critical frequencies and peak density heights over the three days are shown in Figure 5.5 and Figure 5.6 respectively.

There are several important observations from the critical frequencies plot, the first of which is the variations of the F2 critical frequency between 15:00 local-time (LT) and 22:00 LT, which coincided with the period of transmission of the JFAS radar. Thus the variations in f_{oF2} might have had an impact on the fading of the signals during that time.

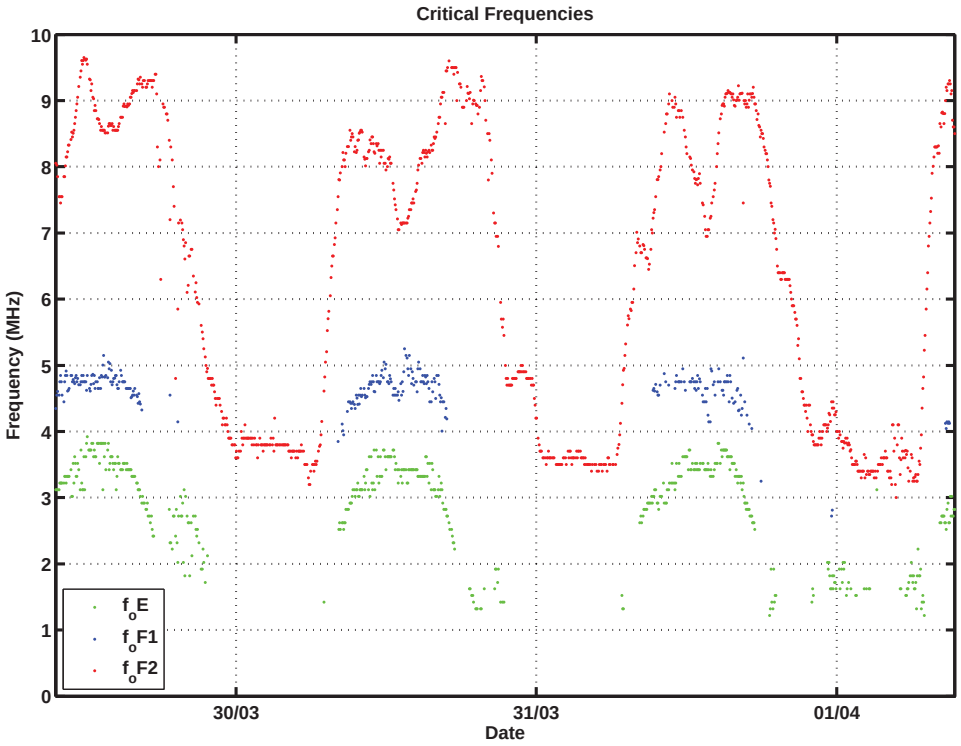

Figure 5.5. The critical frequencies of the three layers - E, F1 and F2, over the time period of the experiment. X-axis markers denote 00:00 local-time of the date specified.

Another interesting observation is the existence of the F1 layer just before sunset, which indicates the possibility of a propagation mode sustained by the F1 layer before the sunset period.

Looking at the peak density heights, one can see the increase in the height of the remaining F2 layer. There were significant variations in the peak density height during the night-time period, however some of the more extreme observations would most likely be due to the measurement noise introduced by the ionosonde itself. Short term fluctuations can also be derived from the ionosonde data (observations at intervals of 3.75 minutes were available). These were used to determine the magnitude of the disturbance that caused the fading in signals.

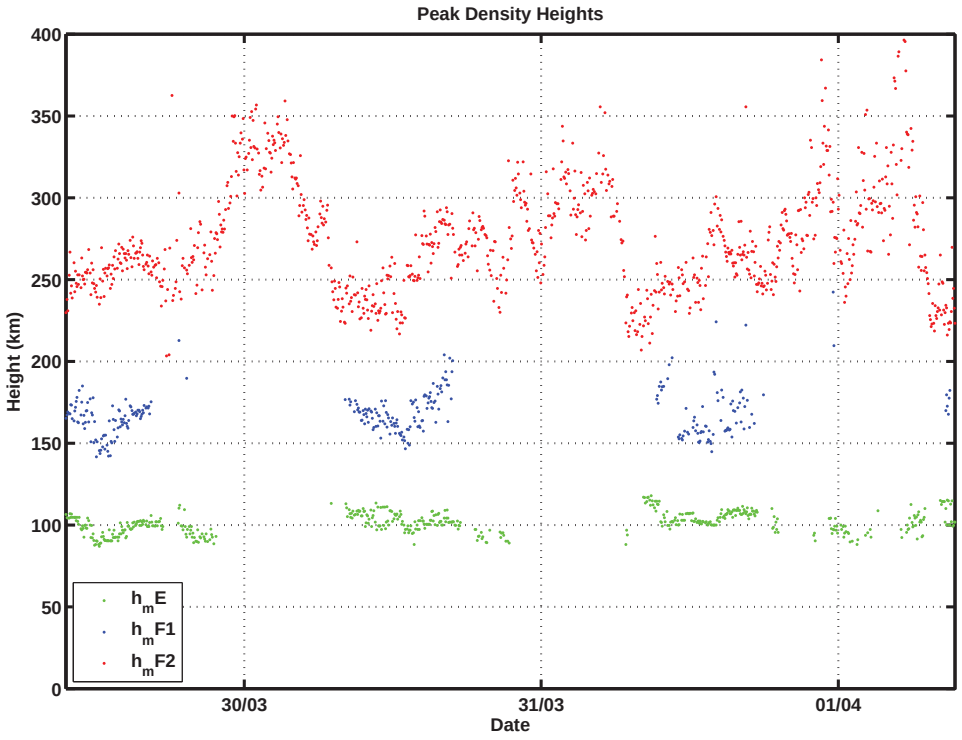

Figure 5.6. Peak heights of the three layers - E, F1 and F2, over the time period of the experiment. X-axis markers denote 00:00 local-time of the date specified.

5.5 Signal Characteristics

The linear FMCW signal waveform, otherwise known as the chirp waveform, is characterised by a linear increase in signal frequency over the sweep period. A single sweep linear FMCW signal with an increasing frequency can be expressed by

$$x(t) = \cos\left(2\pi\left(f_0\, t + \frac{B}{2T_r}\, t^2\right)\right) \qquad -\frac{T_r}{2} \leq t \leq \frac{T_r}{2} \tag{5.1}$$

where f_0 is the centre frequency, B is the bandwidth of the FMCW signal, and T_r is the sweep period. The actual transmitted waveform was a periodic version of the single sweep FMCW signal. The frequency-time characteristics of the transmitted waveform are shown in Figure 5.7.

During the experiment, the JFAS radar transmitter was operating with a waveform repetition frequency (WRF) of 5 Hz, and the corresponding sweep period T_r was 0.2 seconds. The bandwidth B and centre frequency f_0 of the FMCW signal was chosen by the FMS, and they are shown in Table 5.1. A full-sweep cycle lasts for 12.6 seconds, and

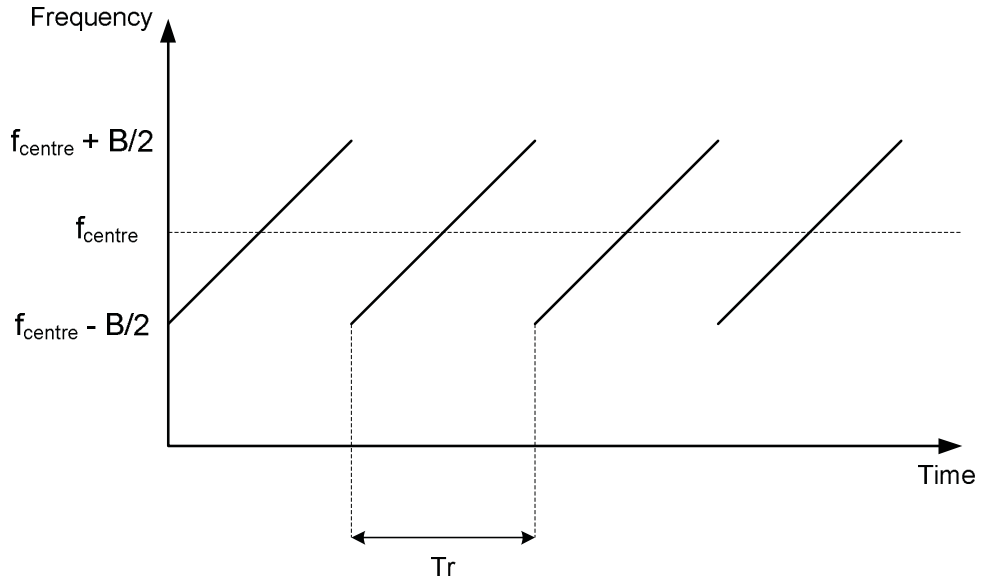

Figure 5.7. Frequency-Time characteristics of a FMCW signal, showing the centre frequency f_0, bandwidth B and sweep period T_r.

repeats itself after a 1.4-second break. A spectrogram of a received FMCW waveform showing the full-sweep cycle and break is shown in Figure 5.8.

For the first two days of the experiment, the JFAS radar transmitter was configured in scanning mode, and therefore the geographic footprint of the radar beam was changing with time. The coverage region as shown in Figure 5.2 was separated into three zones, with the radar beam switching between each geographic area every 14 seconds of the full-sweep cycle plus break. Since the CCP receiver was located at Lake Bennett, there were times when the signal was actually received via the side-lobe of the antenna beam pattern. The scanning mode introduced a constant amplitude offset factor in the received signal. To overcome this problem, the results were power-compensated with an empirically calculated factor at the data processing stage.

5.6 Data Processing and Analysis

To extract the desired information regarding the fading of signals propagating in the ionosphere, suitable data processing software was developed for this experiment. The Data Analysis Module (DAM) was responsible for the off-line processing of the data captured by the CCP. It was specifically designed to extract temporal information on

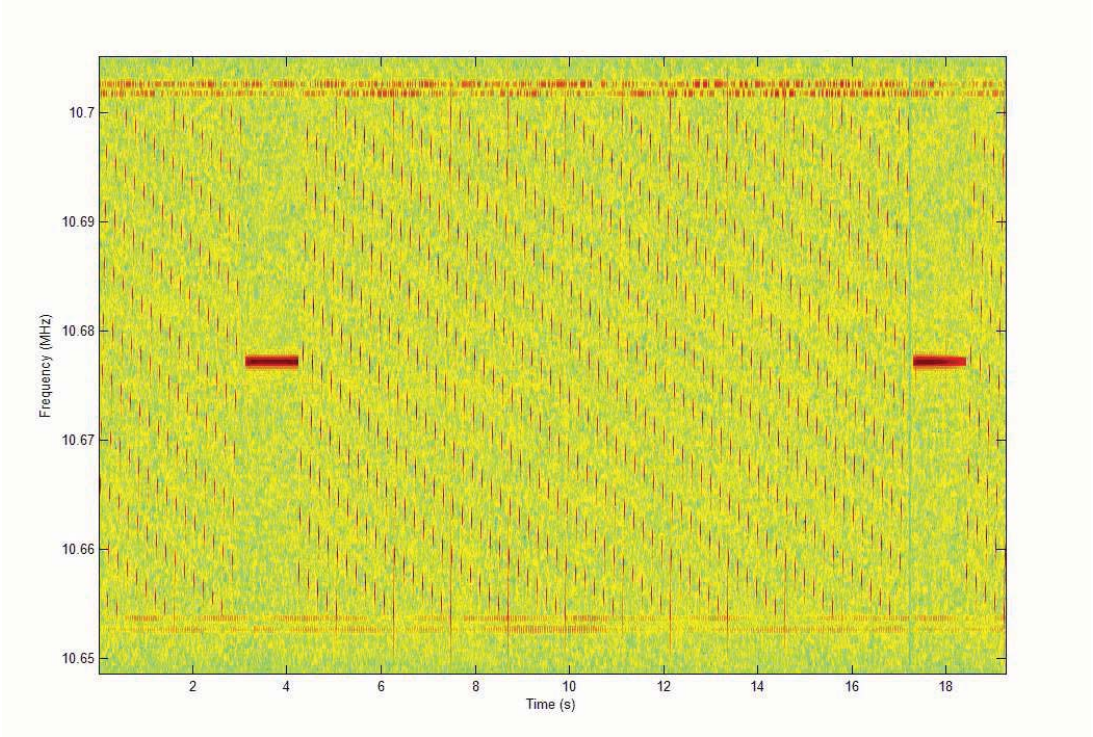

Figure 5.8. Spectrogram of the received FMCW signal at $f_0 = 10.677$ MHz and bandwidth of 46 kHz. Note the 12.6 seconds full-sweep cycle and the 1.4 second break between each cycle.

fading of the received signal, but more importantly to highlight the frequency-selective fading behaviour in ionospheric propagation.

During the experimental period the incoming signals were captured and stored by the CCP for off-line processing. The captured data were of the digitally down-converted (baseband) version of the transmitted FMCW signal as provided by the digital receiver card. Therefore, the main task of the DAM involved the processing of FMCW waveforms and the extraction of signal fading information for the different possible propagation modes.

5.6.1 FMCW Processing

The area of FMCW digital signal processing has been well established for radar applications [42] [85]. The basis of FMCW processing is as follows: The received FMCW waveform, either from a target reflection for a radar or a delay in propagation within

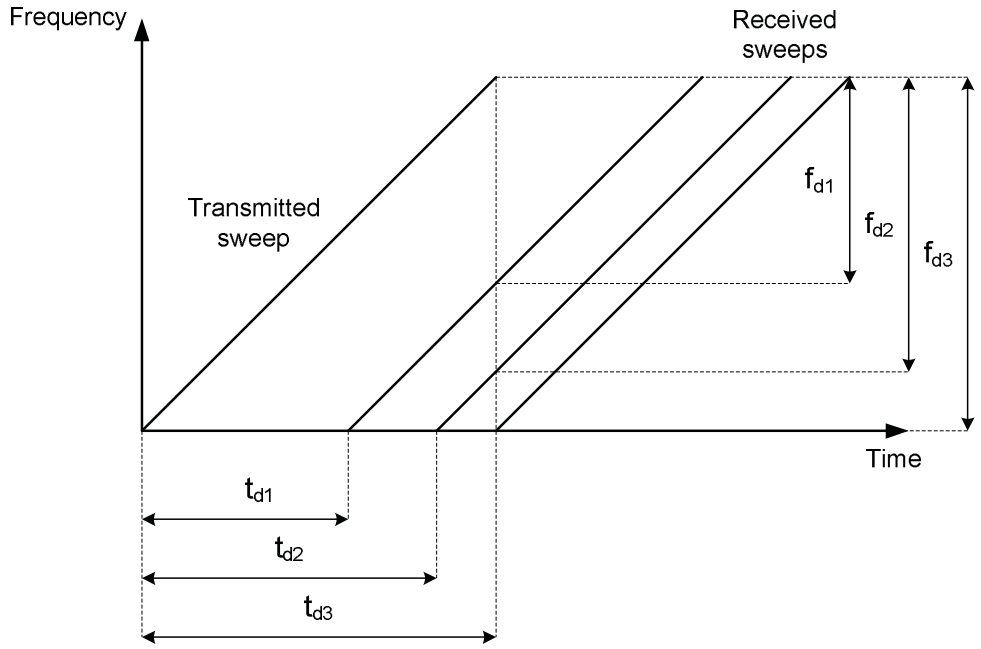

Figure 5.9. Frequency-Time characteristics of the transmitted FMCW signal, and the received sweeps from different propagation modes, showing the time delays t_d and the corresponding frequency shifts f_d produced by the mixing of the received sweeps and the original sweep.

the ionosphere, is mixed with the original transmitted FMCW waveform. This process is commonly known as desweeping or deramping. The mixed signal, after being subjected to low-pass filtering, contains the beat frequency given by

$$f_d = t_d \frac{B}{T_r} \tag{5.2}$$

where t_d is the time delay of the received sweep compared to that of the original transmitted sweep, and B and T_r are as defined in (5.1). The relationships between the time delays and the frequency shifts are illustrated in Figure 5.9. That is, the different time delays of various received modes are translated to frequency offsets that can be easily identified by further spectral analysis.

The DAM makes use of the FMCW processing techniques to identify the different propagation modes and monitor the change in signal amplitude across time and frequency. In all FMCW processing schemes the replica of the original transmitted waveform must be available. This presents a challenging obstacle since neither the actual transmitted FMCW waveform nor any synchronisation data was available at the receiving CCP site.

Consequently, the original transmitted waveform must be carefully synthesised and synchronised by the DAM from the available parameters.

Figure 5.10 shows the various DAM processing stages. The initial processing stages involve the synthesis and synchronisation of the FMCW waveform for the desweeping of the received signal. Particular care was taken to ensure the bandwidth and the sweep period of the synthesised waveform is as close to that of the original transmitted waveform. Otherwise the desweeping process will produce artifacts such as frequency shifts and spurious frequency jumps. Once the desweeping waveform is correctly synthesised, time synchronisation of the desweeping process is then calculated. The purpose of the time synchronisation is so that the time delay of the earliest arrived propagation mode is 0 seconds, i.e. frequency shift of the earliest arrived mode will be 0 Hz. This will be used as reference for comparisons with other received propagation modes.

After the desweeping stage, the resultant signal, or the desweeped waveform, is subjected to further spectral analysis. One would expect the desweeped waveform to contain frequency content that represents the different received modes, starting from the first arrived mode at 0 Hz. To determine the variation of the signal amplitude across the FMCW frequency bandwidth, each 0.2 s cycle of the desweeped signal is broken up into smaller time sections, which essentially contain the signal at different frequencies across the FMCW bandwidth, before a Fourier-transform (FT) is applied. This technique is known as short-time Fourier-transform (STFT) and it is commonly used to analyse the spectral content of a signal as time evolves. As with all FT techniques, special care must be taken to minimise spectral leakage that is caused by the truncation of the sample data. In the current application, spectral leakage has the potential to produce artifacts that can be falsely identified as received modes. To minimise the effects, an appropriate windowing function must be applied to the data samples before applying the FT [86]. The window function used in DAM is the Kaiser-Bessel window as it offers the best compromise between the main-lobe width (mode resolution), and the side-lobe levels (suppression of spurious modes). The actual parameters used for the STFT processing will be presented in the Experimental Results chapter.

The final stages of DAM perform the identification and separation of the different received modes for signal amplitude analysis. Propagation modes are identified by their frequency offset from the first arrived mode. The amplitude correction factor is applied to

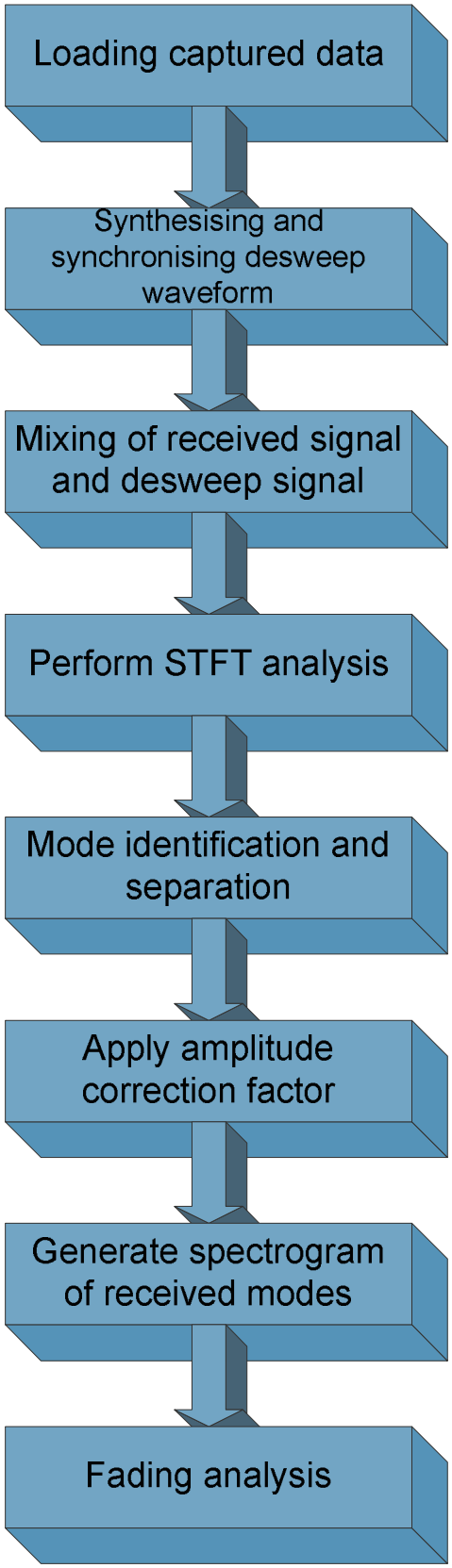

Figure 5.10. Processing stages of the Data Analysis Module (DAM).

the final results to compensate for the effects of the changing geographic footprint of the radar beam. A spectrogram of the different received modes, which shows the variations of signal amplitude across frequency and time, is then generated before fading analysis is applied. Finally, the fading analysis produces metrics such as the rate of fading in time, as well as bandwidth limitations on the signal that are imposed by the frequency-selective fading.

5.6.2 Amplitude-Phase Fading Separation

Although signal fading results from the mode spectrogram can illustrate a clear trend on whether the primary fading mechanism is either amplitude or polarisation, it is possible to separate the two types of fading by simple data manipulation. With two orthogonal receiving antennas connected to the dual-polarisation Compact Channel Probe, the received voltages can be represented by the following:

$$V_H = A(f,t)\cos(\phi(f,t)) \tag{5.3}$$

$$V_V = kA(f,t)\sin(\phi(f,t)) \tag{5.4}$$

where $A(f,t)$ is the amplitude component, $\phi(f,t)$ is the phase component, and k is the constant amplitude offset between the two antennas. The constant amplitude offset factor k is estimated by taking ratio of long time average of voltage amplitudes V_H and V_V:

$$k = \frac{\overline{|V_V|}}{\overline{|V_H|}}. \tag{5.5}$$

After some simple manipulations and rearrangements, the phase and amplitude components are given by:

$$\tan\phi = \frac{V_V}{kV_H} \tag{5.6}$$

$$A^2 = V_H^2(1+\tan^2\phi) \tag{5.7}$$

Using (5.6) and (5.7) one can ascertain the contribution of polarisation and amplitude effects on the overall fading of the signal. The two extreme cases are: If the amplitude

fading component given by (5.7) is varying rapidly, whereas the phase component given by (5.6) is steady, then amplitude fading dominates. Conversely, if the amplitude component is constant, yet the phase varies between 0 and π, then polarisation fading dominates.

It must be noted the above techniques are applied to each received propagation mode. Each mode has a slightly different elevation angle at the transmitter and is transmitted from a different part of the vertical antenna pattern. The constant amplitude correction factor k will be different for each mode and it needs to be calculated separately after all the modes have been identified.

This page is blank